

Chapter 2

Space Robot Control for Unknown Target Handling

Shinichi Tsuda and Takuro Kobayashi

Abstract Space robot is now playing very important role in space activities. Especially in space station a few robot arms are working for construction and repairing. However these robots are so-called remote manipulators operated by astronauts. For future applications the space robot must be autonomous and is expected to maintain the failed satellites and to capture the space debris. This chapter deals with space robot control for unknown target in robust manner. To cope with unknown characteristics the sliding mode control is applied in this study.

Keywords Robust control • Sliding mode control • Space robot • Target handling

1 Introduction

Space robot technology has been rapidly developed and extensively used in the space station program. Most of these space robots are a kind of remote manipulator systems controlled by astronauts from inside or outside of space station. In the space application more intelligent system is desirable to reduce the workload and hazardous risk of those astronauts. Therefore in the near future this technology will be expected to perform the wider range of operations, such as to maintain failed satellites and to capture space debris in the autonomous manner by the space robot.

S. Tsuda (✉)

Department of Aeronautics and Astronautics, School of Engineering, Tokai University,
4-1-1 Kitakaname, Hiratsuka, Kanagawa, 259-1292, Japan
e-mail: stsuda@keyaki.cc.u-tokai.ac.jp

T. Kobayashi

INEC Engineering Limited, Higashi-shinagawa 4-10-27, Shinagawa, Tokyo 140-0002, Japan
e-mail: 9amjm005@mail.tokai-u.jp

This capability will tremendously decrease the extravehicular operations of astronauts, which are most time consuming and terribly exhausting. In this respect the autonomy will be mandatory.

In the space robot operation there are a few features like the reactive behavior of attitude motion of the space robot by robot arm operation and the parameter change in attitude dynamic equations of motion by capturing the target and so on. Generally speaking the failed target and debris will not be accurately known a priori and freely rotating, that is, some of physical parameters are unknown. In the above respect some kind of robustness of the space robot control must be incorporated [1].

This study deals with the space robot operation, i.e., controlling the attitude of the space robot and controlling the robot arm under the changed mass property. The sliding mode control [2] is applied to the control of attitude motion and the robot arm in which the absolute supremum value method [3] was used to assure the robustness.

2 Model of Space Robot

The model of a space robot is illustrated in Fig. 2.1. A robot arm is mounted on the body of the spacecraft. The robot arm is articulated with three rotary joints and the motion of the robot arm is assumed to be two dimensional.

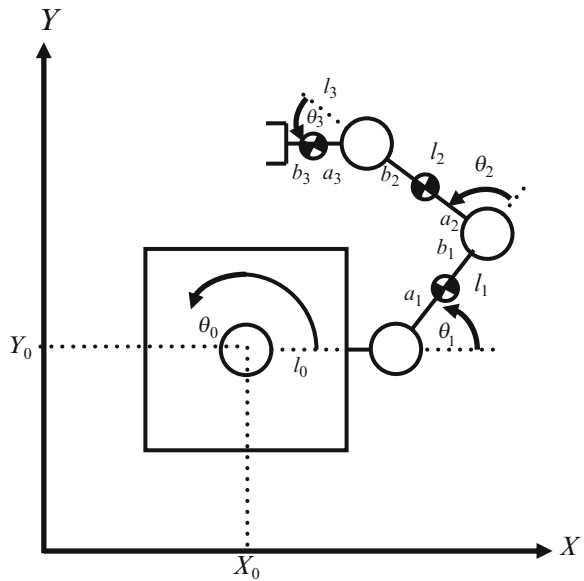


Fig. 2.1 Model of space robot

3 Equations of Motion

Dynamical equations of motion for space robot are derived using Lagrange formula. It will be obtained as follows.

K is the kinetic energy and P is the potential energy, then, Lagrange equations of motion is expressed in the following:

$$Q_{ib} = \frac{d}{dt} \left(\frac{\partial K}{\partial \dot{q}_i} \right) - \frac{\partial K}{\partial q_i} + \frac{\partial P}{\partial q_i}. \quad (2.1)$$

Both energies are given as below:

$$K = \frac{1}{2} m \mathbf{v}^T \mathbf{v} + \frac{1}{2} \boldsymbol{\omega}^T I \boldsymbol{\omega} \quad (2.2)$$

$$P = mgl. \quad (2.3)$$

where m , \vec{v} , $\vec{\omega}$ and I are mass, velocity vector, angular velocity vector and moment of inertia, respectively.

Detailed Geometry of the space robot is illustrated in the Fig. 2.1.

Center of mass for the space robot and each link is given by s_{iX}, s_{iY} ($i = 0, 1, 2, 3$). And the velocity is v_i . a_i expresses the length between the joint and link center of mass, and b_i gives the length between the joint and link center of mass.

Then we have the following relationships:

$$\begin{aligned} s_{0X}(t) &= X_0(t) \\ s_{0Y}(t) &= Y_0(t) \\ v_0(t) &= \dot{s}_{0X}^2(t) + \dot{s}_{0Y}^2(t) \\ s_{1X}(t) &= X_0(t) + l_0 C_0 + a_1 C_{01} \\ s_{1Y}(t) &= Y_0(t) + l_0 S_0 + a_1 S_{01} \\ v_1(t) &= \dot{s}_{1X}^2(t) + \dot{s}_{1Y}^2(t) \\ s_{2X}(t) &= X_0(t) + l_0 C_0 + l_1 C_{01} + a_2 C_{012} \\ s_{2Y}(t) &= Y_0(t) + l_0 S_0 + l_1 S_{01} + a_2 S_{012} \\ v_2(t) &= \dot{s}_{2X}^2(t) + \dot{s}_{2Y}^2(t) \\ s_{3X}(t) &= X_0(t) + l_0 C_0 + l_1 C_{01} + l_2 C_{012} + a_3 C_{0123} \\ s_{3Y}(t) &= Y_0(t) + l_0 S_0 + l_1 S_{01} + l_2 S_{012} + a_3 S_{0123} \quad v_3(t) = \dot{s}_{3X}^2(t) + \dot{s}_{3Y}^2(t) \end{aligned} \quad (2.4)$$

The kinetic energies are described as below:

$$\begin{aligned}
 K_0 &= \frac{1}{2}m_0v_0^2 + \frac{1}{2}I_0\omega_0^2 \\
 K_1 &= \frac{1}{2}m_1v_1^2 + \frac{1}{2}I_1(\omega_0 + \omega_1)^2 \\
 K_2 &= \frac{1}{2}m_2v_2^2 + \frac{1}{2}I_2(\omega_0 + \omega_1 + \omega_2)^2 \\
 K_3 &= \frac{1}{2}m_3v_3^2 + \frac{1}{2}I_3(\omega_0 + \omega_1 + \omega_2 + \omega_3)^2
 \end{aligned} \tag{2.5}$$

The potential energies for free floating bodies on the orbit are given by the following:

$$P_0 = P_1 = P_2 = P_3 = 0 \tag{2.6}$$

Those equations are summarized as in (2.7) by substituting the above relations, where $M(\theta)$ is the inertia matrix and $h(\theta, \dot{\theta})$ includes centrifugal and Coriolis terms. $u(t)$ is translational control force, attitude control and joint control torque vector for space robot.

$$M(\theta)\ddot{q}(t) + h(\theta, \dot{\theta}) = u(t) \tag{2.7}$$

where

$$\begin{aligned}
 q &= [X \ Y \ \theta_0 \ \theta_1 \ \theta_2 \ \theta_3]^T \\
 \theta &= [\theta_0 \ \theta_1 \ \theta_2 \ \theta_3]^T.
 \end{aligned}$$

Further we assume the following relations:

$$M(\theta) = M^0(\theta) + \Delta M(\theta) \tag{2.8}$$

$$h(\theta, \dot{\theta}) = h^0(\theta, \dot{\theta}) + \Delta h(\theta, \dot{\theta}) \tag{2.9}$$

In which $M^0(\theta)$ and $h^0(\theta, \dot{\theta})$ are defined as nominal value matrix and vector, $\Delta M(\theta)$ and $\Delta h(\theta, \dot{\theta})$ are called deference from nominal values and absolute supremum values are defined as bellow;

$$|\Delta M_{ij}(\theta)| \leq \hat{M}_{ij}(\theta) \tag{2.10}$$

$$|\Delta h_i(\theta, \dot{\theta})| \leq \hat{h}_i(\theta, \dot{\theta}). \tag{2.11}$$

And further, absolute supremum values of elements of time derivative $\dot{M}_{ij}(\theta)$ of matrix $M(\theta)$ was also defined in the following manner;

$$|\dot{M}_{ij}(\theta)| \leq \hat{\dot{M}}_{ij}(\theta). \tag{2.12}$$

The absolute supremum value $\hat{v}_i(q, t)$ will be given as follows;

$$|\{M(\theta)\ddot{q}_d(t)\}_i| \leq \hat{v}_i(\theta, t). \tag{2.13}$$

4 Sliding Mode Control

The sliding mode control restricts the trajectory of plant states on a hyper plane by the control and slides it to the equilibrium point in an asymptotic manner.

First let us design the switching hyper plane. The target trajectory is given by q_d and controlling errors are defined by the followings;

$$e(t) = q(t) - q_d(t) \quad (2.14)$$

$$\dot{e}(t) = \dot{q}(t) - \dot{q}_d(t). \quad (2.15)$$

And then we give the switching hyper plane as an (2.10).

$$\sigma(t) = \Lambda e(t) + \dot{e}(t) \quad (2.16)$$

where

$$\Lambda = \text{diag}(\lambda_1, \dots, \lambda_n) \quad \lambda_i > 0.$$

If $\sigma(t) = 0$ holds, then, $e(t)$ in (2.16) satisfies the asymptotic stable differential equation and $e(\infty) \rightarrow 0$ is assured. In order to secure the state is approaching to the hyper plane, the following Lyapunov function is introduced. And the negative definiteness of its time derivative will be proved.

$$V(\sigma) = \frac{1}{2} \sigma^T M \sigma \quad (2.17)$$

The time derivative of (2.17) is given by

$$\begin{aligned} \dot{V} &= \frac{1}{2} \sigma^T \dot{M} \sigma + \sigma^T M \dot{\sigma} \\ &= \frac{1}{2} \sigma^T \dot{M} \sigma + \sigma^T (M \Lambda \dot{e} + M \ddot{q} - M \ddot{q}_d) \\ &= \frac{1}{2} \sigma^T \dot{M} \sigma + \sigma^T (M \Lambda \dot{e} - h + u - M \ddot{q}_d). \end{aligned} \quad (2.18)$$

Let us define $u(t)$ as follows;

$$u(t) = -M^0(\theta) \Lambda \dot{e} + h^0(\theta, \dot{\theta}) - P \sigma - Q \text{sgn}(\sigma) \quad (2.19)$$

where

$$P := \text{diag}(P_{11}(t), \dots, P_{nn}(t)) \quad Q := \text{diag}(Q_{11}(t), \dots, Q_{nn}(t)),$$

then, we obtain

$$\begin{aligned} \dot{V} &= \frac{1}{2} \sigma^T \dot{M} \sigma + \sigma^T [M \Lambda \dot{e} - h - M \ddot{q}_d] \\ &\quad + \sigma^T [-M^0 \Lambda \dot{e} + h^0 - P \sigma - Q \text{sgn}(\sigma)] \end{aligned}$$

$$\begin{aligned}
&= -\sigma^T \left[P - \frac{1}{2} \dot{M} \right] \sigma \\
&\quad + \sigma^T [-Q \operatorname{sgn}(\sigma) + \Delta M \Lambda \dot{e} + \Delta h - M \ddot{q}_d]. \tag{2.20}
\end{aligned}$$

Here we choose P and Q which satisfy $\dot{V}(s) < 0$.

In the first place elements of the diagonal matrix Q are determined as below;

$$Q_{ii}(t) = \sum_{j=1}^n \left\{ \hat{M} \Lambda \right\}_{ij} |\dot{e}_j| + \hat{h}_i + \hat{v}_i. \tag{2.21}$$

Then we have

$$\sigma^T Q \operatorname{sgn}(\sigma) \geq \sigma^T [\Delta M \Lambda \dot{e} - \Delta h - M \ddot{q}_d], \tag{2.22}$$

And the second term of (2.20) becomes negative semi-definite. In the next place if we define elements of diagonal matrix P as follows;

$$P_{ii}(t) = \sum_{j=1}^n \hat{M}_{ij}/2 + k_i, \quad k_i > 0, \tag{2.23}$$

then, the first term $P - \frac{1}{2} \dot{M}$ of (2.20) is given by the following,

$$\frac{1}{2} \begin{bmatrix} \sum_{j=1}^n \hat{M}_{1j} - \dot{M}_{11} & -\dot{M}_{12} & \cdots & -\dot{M}_{1n} \\ -\dot{M}_{21} & \sum_{j=1}^n \hat{M}_{2j} - \dot{M}_{22} & & -\dot{M}_{2n} \\ \vdots & & \ddots & \vdots \\ -\dot{M}_{n1} & -\dot{M}_{n2} & \cdots & \sum_{j=1}^n \hat{M}_{nj} - \dot{M}_{nn} \end{bmatrix} + K. \tag{2.24}$$

By the Gershgorin's theorem, for an arbitrary matrix $A = [a_{ij}]$, if the following inequality is satisfied;

$$a_{ij} \geq \sum_{k=1, k \neq i}^n |a_{ik}| \tag{2.25}$$

then, the matrix A is positive semi-definite. Therefore if we apply $k_i > 0$ to the (2.24), then, we have the negative definiteness of the first term in (2.20). This means $\dot{V} < 0$. The above concludes the proof of the negative definiteness of the Lyapunov function.

And in order to avoid the chattering phenomena, we introduce saturation function in place of sgn function.

$$\operatorname{sat}(\sigma/\varepsilon) = \begin{cases} 1 & \sigma > \varepsilon \\ \sigma/\varepsilon & |\sigma| \leq \varepsilon \\ -1 & \sigma < -\varepsilon \end{cases} \tag{2.26}$$

5 Numerical Simulations

We conducted numerical simulations for the space robot model defined in Fig. 2.1. And to perform the mission two phases are introduced.

5.1 Phase I

To capture the target the robot arm follows the motion of the target for 10 s. By this operation grasping operation will be completed.

In order to realize to follow the target, a goal trajectory $r_d(t)$ for the position of endeffector of the robot arm is defined and then, the joint trajectory for $q_d(t)$ is calculated. The position of the center of target is X_t and Y_t , and the distance between the center of the target and the grasping point is given by r_t . And the target has the rotational motion. Then we have the following relations;

$$r_d(t) = \begin{bmatrix} X_t + r_t \cdot \cos\left(\frac{\pi t}{360} + \frac{3\pi}{2}\right) \\ Y_t + r_t \cdot \sin\left(\frac{\pi t}{360} + \frac{3\pi}{2}\right) \\ \frac{\pi t}{360} + \frac{\pi}{2} \end{bmatrix} \quad (2.27)$$

$$q_d(t) = [0 \ 0 \ 0 \ \theta_{1d} \ \theta_{2d} \ \theta_{3d}] \quad (2.28)$$

5.2 Phase II

After the grasping operation the velocity of the endeffector will be controlled to be 0 [m/s].

To realize the above operation a goal trajectory for the joint velocity is given by linear functions of time which reduce the velocity to 0 [m/s] after the 30 [s]. The joint velocity vector is given by (2.29).

The supremum value is determined by Table 2.1.

$$\dot{q}_d(t) = [0 \ 0 \ 0 \ \dot{\theta}_{1d}(t) \ \dot{\theta}_{2d}(t) \ \dot{\theta}_{3d}(t)] \quad (2.29)$$

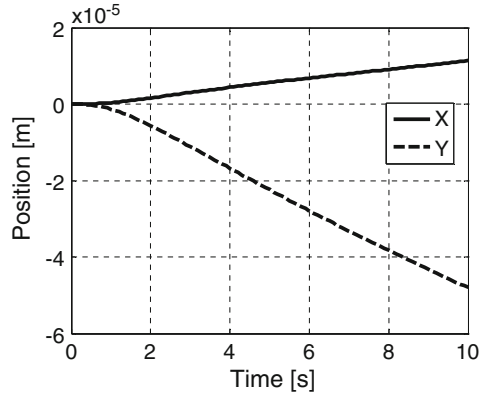
In Table 2.2 parameters for the space robot are defined.

Table 2.1 Parameters of the target

	Target	Assumed value for determining the suremum value
Mass [Kg]	500	600
Moment of inertia [Kgm ²]	333.33	400
Rotational velocity [deg/s]	0.5	0.5
Size	2 [m] × 2 [m]	2 [m] × 2 [m]

Table 2.2 Parameters of the space robot

	Body	Link 1	Link 2	Link 3
Mass [Kg]	1,500	40	40	30
Link length [m]	1.5	1.5	1.5	1.0
Moment of inertia [Kgm ²]	1,000	30	30	10
Initial angle [deg]	0	45	90	-45

Fig. 2.2 History of space robot position for phase 1 operation

Other parameters are assumed as follows;

$$k_1 = k_2 = k_3 = k_4 = k_5 = k_6 = 100$$

$$\lambda_1 = \lambda_2 = 15, \lambda_3 = 10, \lambda_4 = \lambda_5 = \lambda_6 = 5$$

$$\varepsilon_1 = \varepsilon_2 = \varepsilon_3 = \varepsilon_4 = \varepsilon_5 = \varepsilon_6 = 0.05.$$

Some of the above parameters are determined by iterative manner.

Results of the *Phase I* are shown in Figs. 2.2–2.8. The performance of tracking the target is satisfactory and the error of tracking was below 1 [mm].

Results of the *Phase I* are shown in Figs. 2.2–2.8. The performance of tracking the target is satisfactory and the error of tracking was below 1 [mm].

Results of Phase II control are given by Figs. 2.9–2.18.

The control of position and velocity of the space robot is satisfactory and control input for spacecraft position and joint angles is sufficiently small, for instance, the maximum torque for both the space robot attitude control and joint control is smaller than 1 [Nm]. These values are consistent with the space application.

In general mounted thruster forces are from 1 N to 10 N for thousand kg class spacecrafts and typical arm length for the torque will be 2 m or 3 m. Furthermore, typical torque capability by reaction wheel for the attitude control of spacecraft is 1 Nm. These facts validate the applicability of our approach.

Fig. 2.3 History of control force for space robot

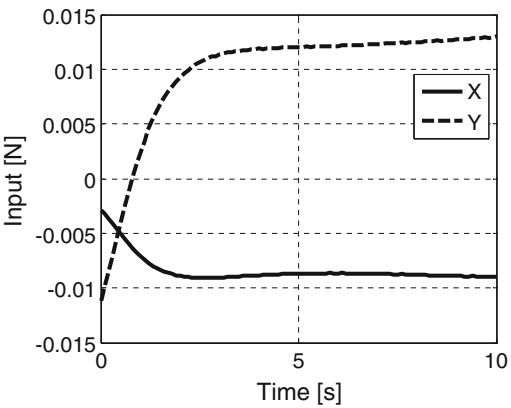


Fig. 2.4 History of space robot attitude angle for phase 1 operation

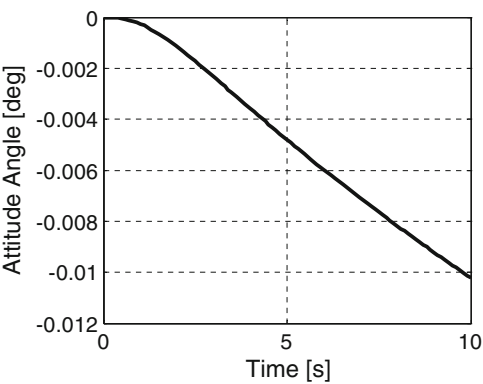


Fig. 2.5 History of control input torque

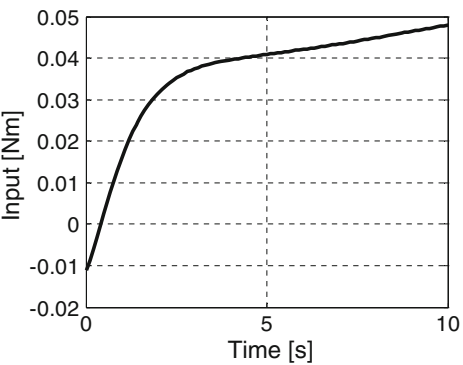


Fig. 2.6 History of joint angles for phase 1 operation

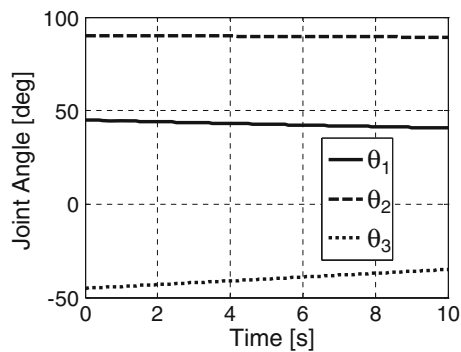


Fig. 2.7 History of desired joint angles

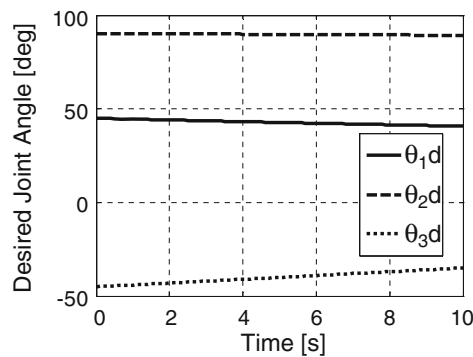


Fig. 2.8 History of joint torque input

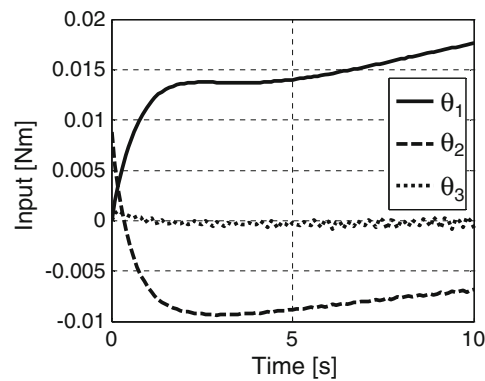


Fig. 2.9 History of space robot position

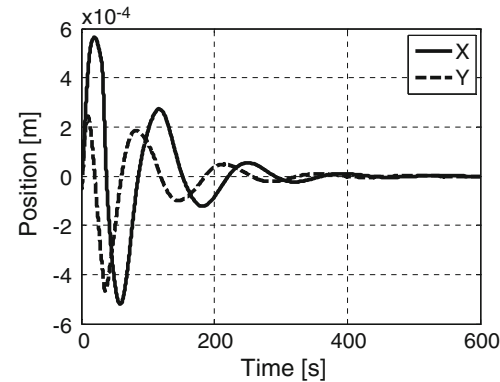


Fig. 2.10 History of space robot velocity

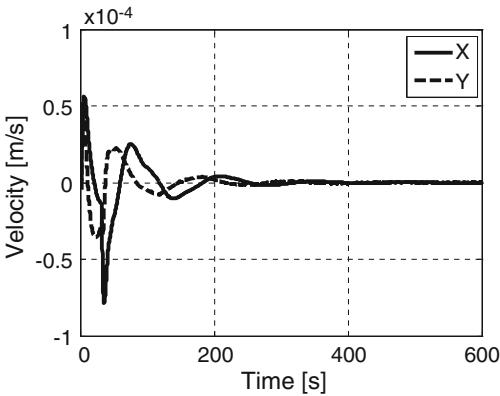


Fig. 2.11 History of translational control input

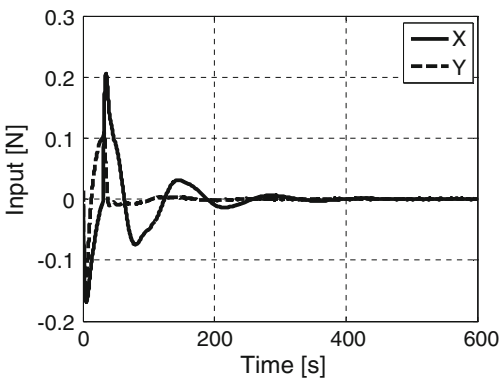


Fig. 2.12 History of space robot attitude angle

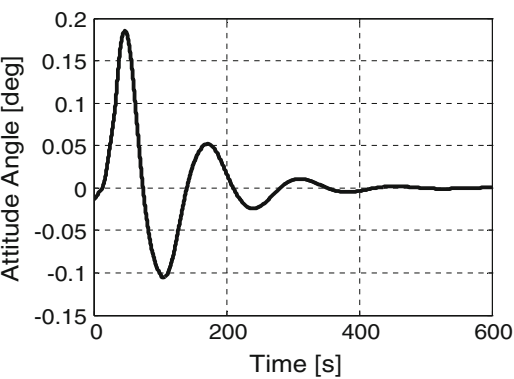


Fig. 2.13 History of attitude angle velocity

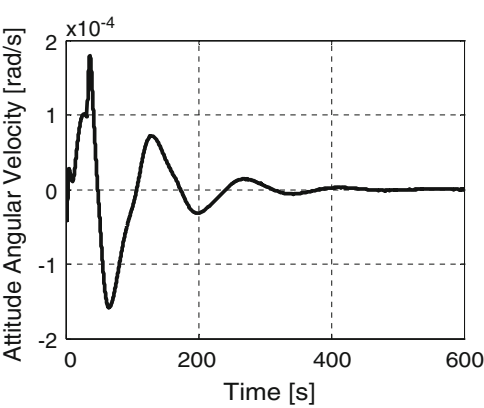


Fig. 2.14 History of torque control input for space robot

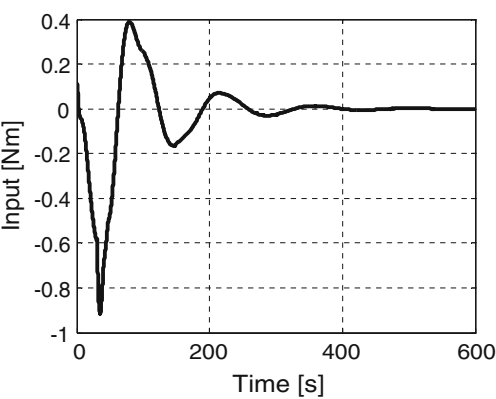


Fig. 2.15 History of joint angles for space robot

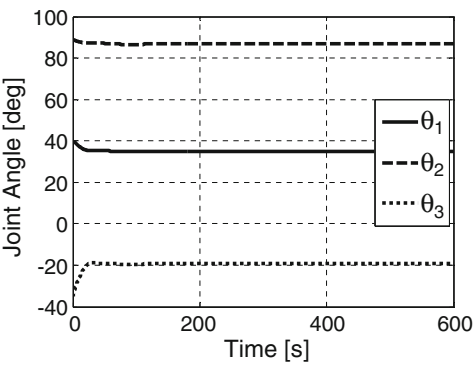


Fig. 2.16 History of desired joint velocities

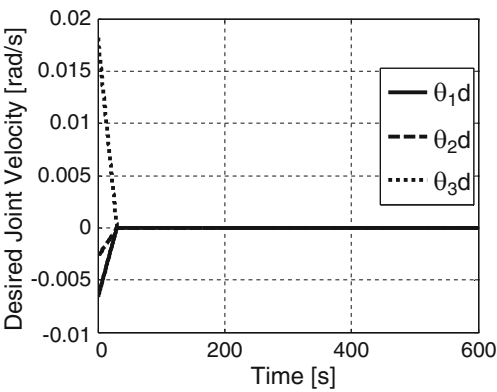


Fig. 2.17 History of joint angles

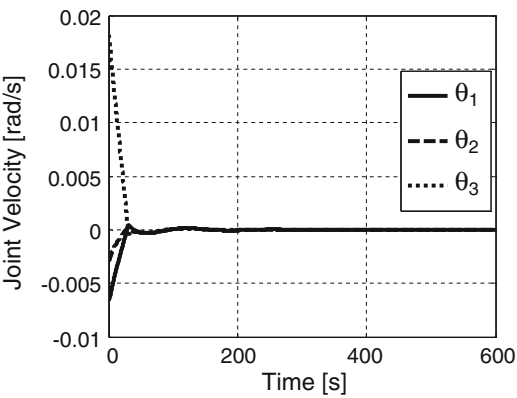
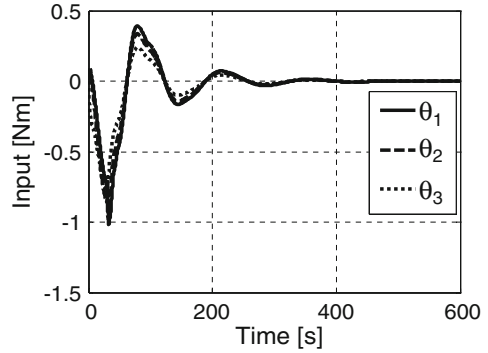


Fig. 2.18 History of control torque input



6 Conclusion

In this study robust control of space robot for unknown target capturing operation was discussed. The target initially has freely rotating motion, therefore we defined two phases, in which we have operations of grasping the target and stabilizing both the space robot and the target. The sliding mode control was applied to have the robustness of control. Numerical simulations were conducted and the results show the consistency with space application requirement. This validates our approach.

References

1. Kobayashi T, Tsuda S (2011) Robust control of space robot for moving target capturing, Lecture notes in engineering and computer science: proceedings of the international multiconference of engineers and computer scientists, IMECS 2011, 16–18, Hong Kong, pp 834–838
2. Noba K, Den H (1994) Sliding mode control. Corona, Tokyo
3. Mita T, Chin G (1990) Sliding mode control and trajectory control of robot arm. System Control Inform 34(1):50–55



<http://www.springer.com/978-1-4614-1694-4>

Intelligent Control and Innovative Computing

Ao, S.I.; Castillo, O.; Huang, H. (Eds.)

2012, X, 438 p., Hardcover

ISBN: 978-1-4614-1694-4